Advanced Parallel Imaging Techniques for Metabolic Imaging with Hyperpolarised 13C

R. F. Schulte[1], J. I. Sperl[1], A. Haase[2], M. Irkens[3], M. Manglberger[3], E. Weidl[4], G. Kudielka[1], M. Schwaiger[4], and F. Wiesinger[1]
[1]GE Global Research, Munich, Germany, [2]IMETUM, Technische Universitaet Muenchen, Munich, Germany, [3]Rapid Biomedical, Würzburg, Germany, [4]Department for Nuclear Medicine, Technische Universitaet Muenchen, Munich, Germany

Introduction

Metabolic imaging of hyperpolarised [1-13C]pyruvate and its downstream metabolites lactate, alanine and bi-carbonate requires efficient acquisition sequences with sufficient spatial and some spectral encoding to resolve the (sparse) spectra. The magnetisation is irreversibly depleted by T_1 decay and repetitive excitation, hence placing tight constraints onto the acquisition. Parallel imaging methods increase encoding efficiency by utilising spatial coil information in the encoding and reconstruction process [1-3], are widely used for normal proton imaging, and are believed to form a particularly synergistic combination with hyperpolarised imaging [4,5]. Objective of this work was to implement and investigate parallel imaging for non-Cartesian hyperpolarised 13C CSI in the form of IDEAL spiral CSI encoding [6] and to compare different reconstruction techniques.

Theory and Methods

Various chemical-shift imaging (CSI) methods are currently being used for hyperpolarised 13C metabolic imaging. Regular sequential pulse-and-acquire based CSI (FIDCSI) is inefficient but well-suited for demonstrating proper parallel imaging unfolding of undersampling artefacts, which is often difficult to see with non-Cartesian trajectories. For parallel imaging, the FOV was reduced to 4×4cm^2 and reconstructed to 8×8cm^2 with a matrix size of 12×12 (144 excitations, 5° flip angle, TR=75ms, slice thickness=1cm). For comparison to an efficient sequence with a dynamic (temporally resolved) acquisition, IDEAL spiral CSI was chosen [6] for a second pyruvate injection in the same animal. Eight excitations are required for encoding one CSI data set, using one pure spectral acquisition and seven single-shot spirals acquired with seven different TEs (ΔTE=1.12ms). A 65ms-duration, variable-density single-shot spiral trajectory was designed starting with two-fold oversampling in the centre with smooth transition to four-fold undersampling at the edge of k-space, a nominal matrix size of 36×36 and FOV=8×8cm^2 (10° flip angle, TR=250ms, slice thickness=1cm). Receive coil sensitivity maps were measured in a separate phantom setup (glas sphere filled with 4M [1-13C]acetate doped with 1:100 ProHance) using the same prescription with a 16×16 FIDCSI encoding (TR=1s).

Experiments were performed on a GE Signa HDx 3T scanner (GE Healthcare, Milwaukee, WI, USA) equipped with a custom-made 7cm inner diameter 1H/13C dual-tuned transmit (TX) – receive (RX) coil arrangement, composed of a TX-RX quadrature 1H birdcage coil, a TX-only quadrature 13C birdcage coil and a volumetric four-channel 13C RX-only coil consisting of 6cm elements in circumferential direction (Rapid Biomedical, Würzburg, Germany). [1-13C]Pyruvic acid was polarised for ~1hr and rapidly dissolved in a HyperSense DNP polariser (OxfordInstruments, Oxford, UK). Healthy male buffalo rats received two 2.5ml/kg 80mM physiological pyruvate injections in the tail vein with imaging starting 20s after (FIDCSI) and prior to injection begin (dynamic IDEAL spiral CSI). The data were transferred and reconstructed off-line using Matlab (The Mathworks, Natick, MA, USA). Phantom sensitivity maps were smoothed, zero-filled to 64×64 and reconstructed by 3D FFT and peak search (Fig 1).

The in-vivo metabolic data were (step 1) spectrally reconstructed to the present chemical-shifts (CS) of pyruvate, pyruvate-hydrate, alanine, lactate and bi-carbonate by CS modelling (matrix inversion) [6]. For Cartesian FIDCSI data, spatial reconstruction (step 2; a) was done by 2D FFT and standard SENSE unfolding using the separately acquired sensitivity maps [1]. For IDEAL spiral CSI, the CS-resolved metabolite data (after step 1) were spatially reconstructed in three different ways (step 2): (b) gridding reconstruction with root-of-sum-of-squares (rsos) coil combination of the individual images; (c) conjugate-gradient (CG) SENSE [2] solving the whole encoding matrix and yielding a combined image; (d) auto-calibrated SPIRiT reconstruction with rsos coil combination [3].

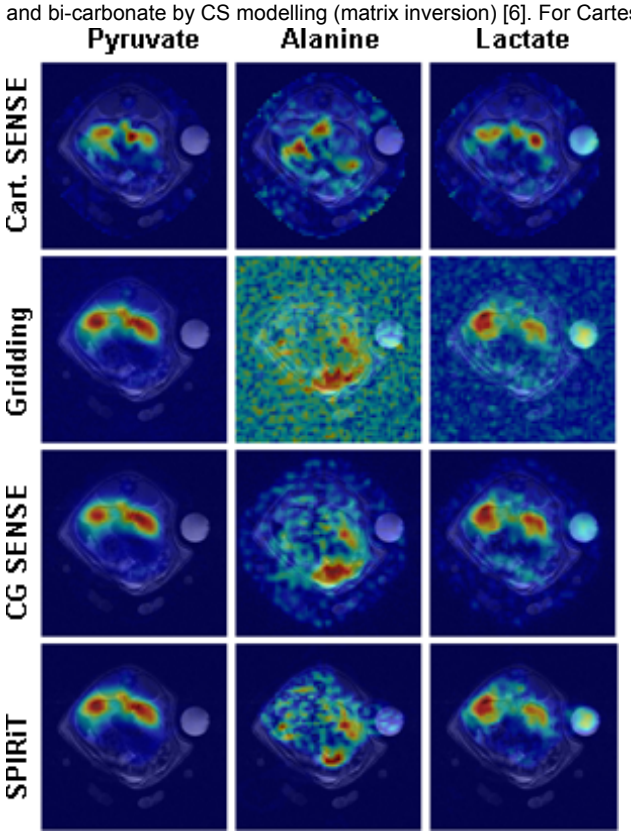

Fig 2: Comparison of parallel imaging reconstructions applied to metabolic data of the kidney.

Results and Discussion

Exemplary in-vivo metabolic images for the different reconstruction methods are shown in Fig 2. The RX coil sensitivity maps show well-separated coil profiles indicating good decoupling performance (Fig 2). While the FIDCSI dataset was used for Cartesian SENSE reconstruction (Fig 2 top), the IDEAL spiral CSI dataset and its pre-processing was always the same for the other methods. Time steps #5 to #12 out of 32 show sufficient SNR and #7 was chosen for the comparison. The FIDCSI data reconstructed with Cartesian SENSE (top) show some differences in patterns, mainly due to its long overall acquisition and hence time-averaged metabolic distribution. The patterns of the spiral CSI data metabolic images look similar for the gridding, CG SENSE and SPIRiT reconstructions, while a denoising is visible particularly for low SNR metabolite maps such as alanine. In the two SENSE reconstructions, the coils are already SNR-optimally combined [1,2], while gridding and SPIRiT induces some coil weighting through rsos coil combination. The main advantage of SPIRiT however is its auto-calibration, hence obviating the need for a separate coil-sensitivity measurement, while at the same time exhibiting the best SNR. The data is undersampled in high spatial frequencies, where aliasing artefacts rather show up as noise and not as coherent folding, which is reduced by parallel imaging.

References
[1] KP Pruessmann, *et al*. MRM 1999;42:952.
[2] KP Pruessmann, *et al*. MRM 2001;46:638
[3] M Lustig, *et al*. MRM 2010;64:457.
[4] RF Lee, *et al*. MRM 2006;55:1132.
[5] A Arunachalam, *et al*. NMR Biomed 2009;22:867.
[6] F Wiesinger *et al*. ESMRMB 2009;94.

Acknowledgements
This work was partly funded by BMBF MobiTUM grant number 01EZ0826/7.

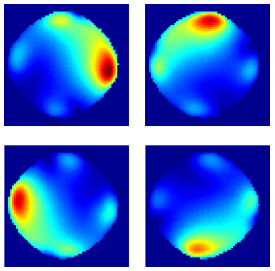

Fig 1: Rx coil sensitivities.